PIBB 生物化学与生物物理进展
Progress in Biochemistry and Biophysics
2023, 50(2): 334~345
www.pibb.ac.cn

Comparative Proteomic Study on The Lesional and Non-lesional Epidermis From Vitiligo Patients*

Ailikemu Tuerxun [1,2,3], CHEN Xiu-Lan[2,3], Ainiwaer Talifu[4], LI Na[2,3], WANG Ji-Feng[3], CAI Tan-Xi[2,3], GUO Xiao-Jing[2,3], DING Xiang[3], XIE Zhen-Sheng[3], NIU Li-Li[3], ZHANG Meng-Meng[3], Ghulam Abbas[2,3], Haji Akber Aisa[1,2)**], YANG Fu-Quan[2,3)**]

([1)]*Key Laboratory of Plant Resources and Chemistry of Arid Zone, Xinjiang Technical Institute of Physics and Chemistry, Chinese Academy of Sciences, Urumqi* 830011, China;
[2)]*University of Chinese Academy of Sciences, Beijing* 100049, China;
[3)]*Laboratory of Protein and Peptide Pharmaceuticals and Laboratory of Proteomics, Institute of Biophysics, Chinese Academy of Sciences, Beijing* 100101, China;
[4)]*Hospital of Xinjiang Traditional Uyghur Medicine, Urumqi* 830049, China)

Graphical abstract

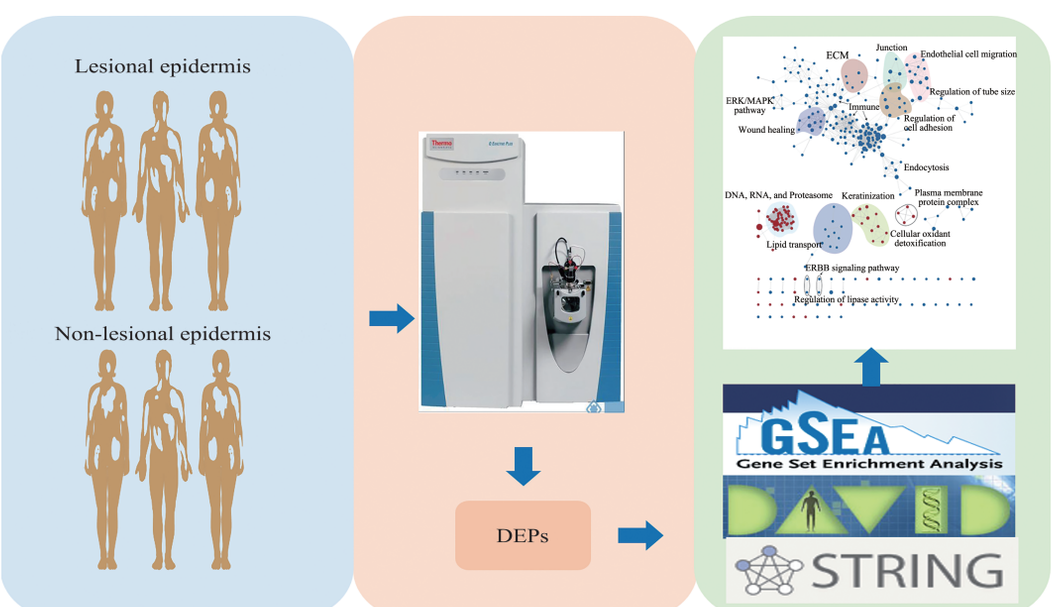

Abstract **Objective** The comparative proteomic study on the paired lesional epidermis (LE) and non-lesional epidermis (NLE) from vitiligo patients to identify the differentially expressed proteins (DEPs) between LE and NLE, and to further explore the molecular mechanism of pathogenesis of vitiligo. **Methods** Firstly, the in solution digestion condition for proteins from epidermis were optimized to sequential tandem digestion with Lys-C and trypsin. Secondly, tandem mass tag (TMT) based quantitative

* This work was supported by a grant from the National Key R&D Program of China (2020YFE0205600).
** Corresponding author.
YANG Fu-Quan. Tel: 86-10-64888581, E-mail: fqyang@ibp.ac.cn
Haji Akber Aisa. Tel: 86-991-3835679, E-mail: haji@ms.xjb.ac.cn
Received: April 11, 2022 Accepted: May 9, 2022

proteomic strategy was performed to compare the proteome profile of the paired LE and NLE from three stable non-segmental vitiligo subjects, and differential expressed proteins (DEPs) were identified. At last, the functional enrichment analysis was performed *via* bioinformatics tool and database (GO, KEGG, STRING, GSEA). **Results** The optimal sequential tandem digestion condition was the combination of Lys-C (enzyme ： substrate, 1 ： 100) and trypsin (enzyme ： substrate, 1 ： 50). A total of 4 496 proteins were identified, and of which 181 were DEPs between LE and NLE from vitiligo patients. Bioinformatics analysis showed that DEPs were mainly related with metabolism, immunity, redox and cell adhesion. Among them, the 119 up-regulated proteins are mainly involved in the processes of keratinization, transcription, oxidative stress, and proteolysis. The 62 down-regulated proteins are mainly involved in intracellular transport, glutathione metabolism and actin filament capping. **Conclusion** The comparative proteomic study revealed that there were functional differences in keratinization, immunity, lipid metabolism and redox between LE and NLE in vitiligo patients. PRDX1, PRDX2, EEF2, ITGB1, SPTBN2, ANXA1 and PFKL were found as the key proteins to disfunction of LE.

Key words vitiligo, epidermal proteomics, TMT labeling, keratinization, oxidative stress, lipid metabolism
DOI：10.16476/j.pibb.2022.0158

Vitiligo is a common depigmenting skin disorder, characterized by patchy skin bordered milky-white depigmentation accompanied by melanocytes disappearance from lesional skin. The worldwide prevalence is between 0.5%−2% without any significant difference in sex, ethnicity, and geographic region. Vitiligo is not life-threatening but influences the quality of life[1-2]. Vitiligo is a multifactorial disorder and there are many hypotheses about the pathogenesis of vitiligo, including genetics, autoimmune, oxidative stress, melanocyte adhesion, and neural factors[3-4]. However, none of these hypotheses clearly explained the mechanism of the pathogenesis of vitiligo.

Quantitative proteomics is an excellent large-scale screening tool for the discovery of the differential expressed proteins (DEPs) and thus could provide a better understanding of the entire protein network[5-7]. However, only the two-dimensional gel electrophoresis (2D-GE) and matrix-assisted laser desorption/ionization time-of-flight mass spectrometry (MALDI-TOF-MS) based proteomic strategy has been used to identify the DEPs in the serum of vitiligo patients[8-9] in the previous proteomics studies on vitiligo. So far, proteomic study on lesional epidermis of vitiligo patients has not been reported.

In this study, in order to identify the features of pathological changes of the lesional epidermis deprived of melanocytes in vitiligo patients, and to explore the molecular mechanism of pathogenesis of vitiligo, TMT-based quantitative proteomic strategy was used to compare the proteome profile of the paired LE and NLE lesional epidermis collected from three stable non-segmental vitiligo patients to identify the DEPs (Figure 1).

1 Materials and methods

1.1 Sample collection

Vitiligo was diagnosed based on the patient’s medical history and typical clinical features (lesions location, size, distribution) by experienced dermatologists accompanied by the Wood’s lamp. The patients with non-segmental vitiligo (NSV) were chosen as participants. The criteria for the patients chosen in this study was based on two conditions: (1) no expansion on preexisting lesions, absence of new lesions and without Koebner phenomenon for at least six months; (2) no external or systemic treatment of vitiligo for at least three months. All participants signed an informed written consent form before the study was initiated. BFY-10 dermis-epidermis separator (negative pressure ranging from 40 to 60 kPa, suction cup with inner diameter of 0.8 cm) was used to induce suction blister. Epidermis was obtained from the center of lesional skin and the paired non-lesional skin (at least 15 cm away from the border of the lesional skin) from the same patient. The six paired epidermis samples from three patients were collected in the Department of Dermatology, Hospital of Xinjiang Traditional Uyghur Medicine.

1.2 Protein extraction from the epidermis

Epidermis samples were washed twice with 500 μl ice-cold phosphate-buffered saline (PBS) and homogenized (OMNI TH-02, US) in 300 μl lysis buffer (6 mol/L urea, 2 mol/L thiourea, 100 mmol/L HEPES, pH 8.5) and 1% protease inhibitor (Roche, cocktail) for 2 min on ice followed by sonication (Scientz-IID, China) for 10 min on ice-water mixture.

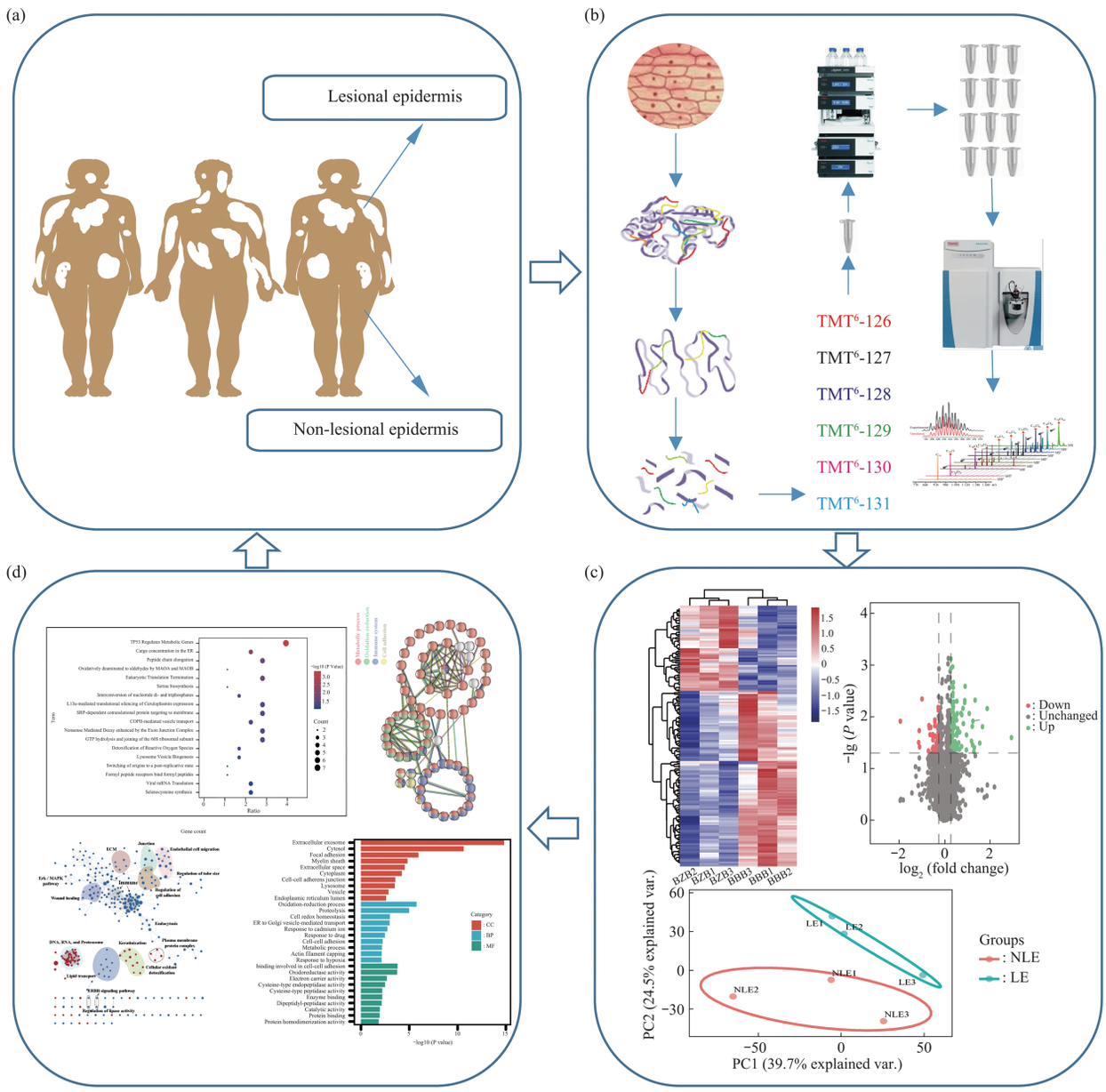

Fig. 1　Schematic illustration of workflow of proteomic analysis

(a) Sample collection; (b) sample preparation and LC-MS/MS analysis; (c) proteomic data exhibition; (d) bioinformatic analysis.

The lysate was centrifuged at 20 000×*g* at 4℃ (Eppendorf, centrifuge 5424 R) for 10 min. The supernatant was collected and stored at −80℃ for further use. The Bradford assay was used to determine the total protein concentration.

1.3　In solution digestion and desalting

All details and data about the optimization of in-solution digestion conditions for epidermis proteins are in the supplementary materials (Figure S1, File S1, Table S1). 50 μg of extracted proteins was taken from each sample and reduced in 10 mmol/L dithiothreitol (DTT) at 37℃ for 1 h, while alkylated in 20 mmol/L iodoacetamide (IAM) for 30 min in the dark, at room temperature. After that, Lys-C (Wako, Japan) was added into the sample solution at a ratio (enzyme/substrate) of 1∶100 (*w*/*w*) and incubated at 37℃ for 3 h. Then, the sample solution was diluted for five folds with 50 mmol/L NH_4HCO_3, and trypsin (Promega) was added at a ratio (enzyme/substrate) of 1∶50 (*w*/*w*) and incubated at 37℃ overnight. Formic

acid (FA) was then added into the sample solution at a final concentration of 0.5% to stop the digestion. The tryptic peptide samples were desalted with HLB C18 columns (Waters, MA, USA), and lyophilized with vacuum centrifugation (LABCONCO).

1.4 TMT 6−plex labeling

All the peptide samples were dissolved in 100 mmol/L TEAB buffer, and 35 μg peptides were taken from each sample solution and labeled with TMT 6-plex reagent (RF232465, Thermo Fisher Scientific, USA) according to the manufacturer's protocol. TMT126-128 reagents were used to label the NLE samples, and TMT129-131 reagents were used to label the LE samples. After labeling, the TMT 6-plex-labeled peptide samples were pooled, desalted, and dried for the next high pH reversed-phase fractionation.

1.5 High pH reversed−phase fractionation

High pH revered-phase (RP) fractionation was carried out to reduce sample complexity and increase the depth of proteome identification as described previously[10]. Briefly, the TMT 6-plex-labeled peptide samples were dissolved in buffer A (2% ACN/98% H_2O, pH=10, adjusted with ammonium hydroxide) and loaded onto an XBridge C18 basic reversed-phase LC column (100 mm×2.1 mm, 3.5 μm particles, Waters). Peptides were separated in a Rigol L-3000 LC system with a binary buffer system of buffer A and buffer B (98% ACN/2% H_2O, pH=10) at a gradient (5%−8% B, 0−5 min; 8%−18% B, 5−40 min; 18%−32% B, 40−62 min; 32%−95% B, 62−64 min; 95%−95% B, 64− 68 min; 95%−5% B, 68−69 min; 5%−5% B, 69−76 min) at a flow rate of 0.2 ml/min). A total of 42 fractions were collected and combined into 12 fractions. These combined fractions were dried and desalted for LC-MS/MS analysis.

1.6 LC−MS/MS analysis

All peptide samples were analyzed on EASY-nLC 1000 system (Thermo Fisher Scientific) coupled with a Q Exactive mass spectrometer (Thermo Fisher Scientific). All peptide samples were dissolved in 0.1% FA and loaded onto an in-house packed capillary RP trap column (100 μm ID×2 cm, Reprosil-Pur C18 AQ, 5 μm, Dr. Maisch GmbH), and separated with a capillary RP C18 column (75 μm ID×20 cm, Reprosil-Pur C18 AQ, 3 μm, Dr. Maisch GmbH) with buffer A (0.1% FA) and buffer B (100% ACN/0.1% FA) at a gradient (4%−12% B, 0−5 min; 12%−22% B, 5−55 min; 22%−32% B, 55−67 min; 32%−90% B, 67−68 min; 90%−95% B, 68−75 min). The flow rate was set to 310 nl/min. Peptide elutates from the column were directly introduced into the mass spectrometer with a spray voltage of 2.0 kV and a capillary temperature of 320°C.

The mass spectrometer was operated in a data-dependent (DDA) mode, MS1 scans at a resolution of 70 000 with an automatic gain control target of 3×10^6 ions and a maximum ion injection time of 60 ms. The top 20 most abundant peaks were selected for fragmentation with an isolation window of 2 *m*/*z* and were fragmented by higher-energy collisional dissociation with a normalized collision energy of 27%. Fragmentation spectra were acquired at a resolution of 17 500 with a target value of 5×10^4 ions and a maximum ion injection time of 80 ms. To minimize peptide re-sequencing, dynamic exclusion was enabled within a time window of 40 s.

1.7 Database searching

Proteome Discoverer software (v2.2) with SEQUEST HT search engine was used for protein identification. Reporter ion intensity was used for protein quantification. MS/MS spectra were searched against Uniprot human-reviewed database (retrieved on December 21, 2020) supplemented with known contaminants. Peptide mass and fragment mass tolerances were set at 10 ppm and 0.02 u, respectively, and a maximum of 2 miss-cleavages were allowed. Cysteine carbamidomethylation, TMT 6-plex labeled lysine (K) and N-terminus of peptides were set as fixed modifications, and N-terminal acetylation on proteins, methionine oxidation were set as variable modifications. Peptide identifications were filtered at a 1% false discovery rate and only high confident peptides were accepted for further analysis.

1.8 Bioinformatics analysis

High confident quantified proteins were used for further analysis. Statistical analysis was performed with paired two-sample Student's *t*-tests. Proteins with fold change (FC) (LE compared to NLE) of more than 1.2 (up-regulated) or less than 0.83 (down-regulated) with P value<0.05 were considered as DEPs. Network analysis of DEPs was performed with DAVID Bioinformatics Resources 6.8 (the total genes in the genome as a background) and STRING (Version 11.5). Gene set enrichment analysis was performed with GSEA 4.1.0 and the terms with false

discovery rate (*FDR*) < 0.05 were visualized with Cytoscape (Version: 3.8.2).

2　Results

2.1　Optimization of protein digestion condition

The protein digestion condition was optimized by comparing four different digestion protocols with combination of Lys-C and trypsin at different ratio of enzyme/substrate. More suitable length of peptides with less missed cleavage under the Lys-C and trypsin sequential digestion protocols (protocols 1, 2, 3) than trypsin digestion alone (protocol 4). The optimized digestion condition protocol 1 (Lys-C 1∶100 + trypsin 1∶50) could achieve the best identification results with 18%−36.4% increase of more proteins identified compared with other conditions (Figure S2).

2.2　Identification of DEPs

TMT-based quantitative proteomic technology was utilized to compare protein expression between LE and NLE of vitiligo patients. A total of 4 496 proteins were identified from TMT-labeled samples. 3 736 proteins, which had quantification information in all the six channels, were selected for further analysis. 181 proteins were regarded as DEPs, with 119 up-regulated and 62 down-regulated (Figure 2a). Principal component analysis (PCA) of these DEPs showed a clear separation with distinct features between LEs and NLEs (Figure 2b).

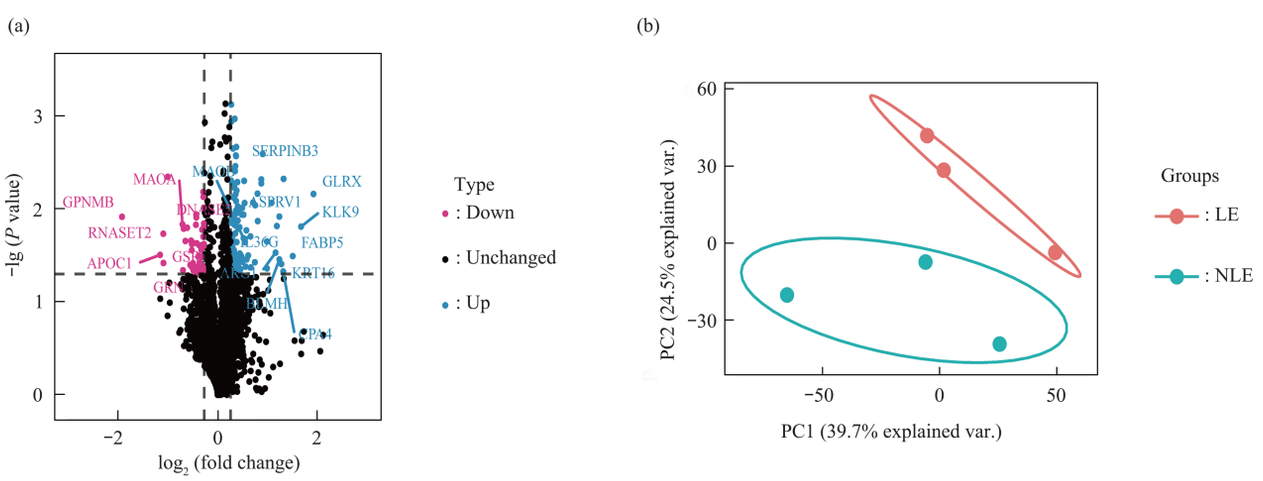

Fig. 2　Comparison of LE and NLE on proteins quantified in epidermis proteomics

(a) Volcano plot of differential protein profiles in the comparison of LE and NLE. Each point representing a single protein. Red for down-regulated protein. Blue for up-regulated protein. (b) Each group was clustered together in the principal components analysis (PCA). Red represents the sample of LE. Blue represents sample of NLE.

2.3　DEPs enrichment analysis

Using GO analysis in DAVID Bioinformatics Resources, functional enrichment of the DEPs was categorized with biological process (BP), cellular component (CC), and molecular function (MF). As shown in Figure 3, for the up-regulated proteins, the top 10 significantly enriched BP were associated with the proteolysis, neutrophil degranulation, translation, cornification (keratinization), cellular response to oxidative stress, and cadmium ion. The CC analysis showed these proteins were enriched in extracellular parts including exosome and extracellular region, followed by cytosol, granular lumen, focal adhesion, lysosome, and endoplasmic reticulum. For MF analysis, these proteins were associated with peptidase and inhibitor activity, followed by oxidoreductase activity, binding, and transferase activity.

For down-regulated proteins, the enriched BP terms included neutrophil degranulation, intracellular transport, actin filament capping, glutathione metabolic process, and response to calcium ion. The enriched CC terms were extracellular region with exosome focal adhesion and membrane, followed by the cortical actin cytoskeleton, granular lumen, and neuronal cell body. The MF predominantly enriched

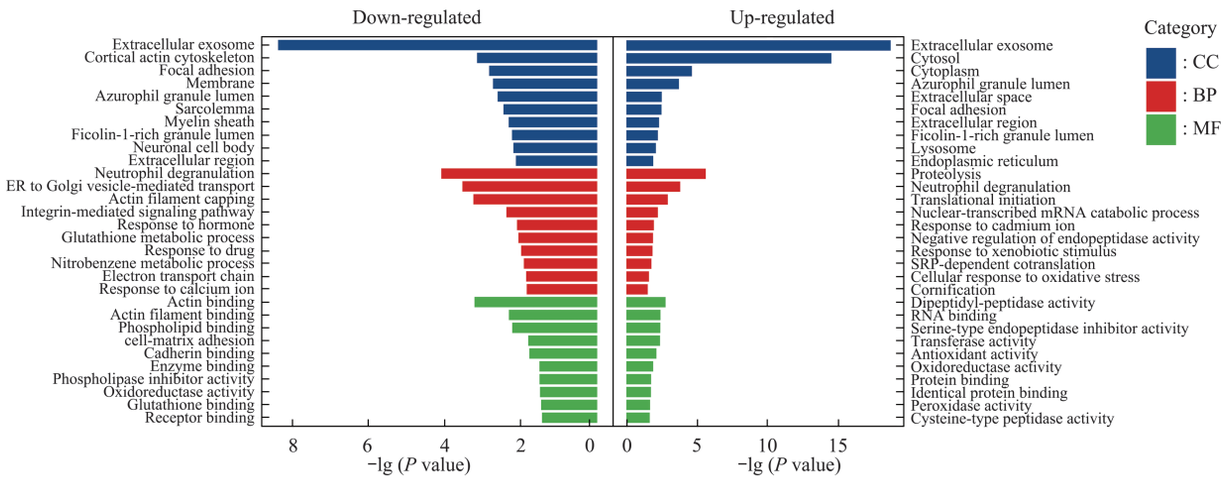

Fig. 3　GO analysis of DEPs in epidermis of vitiligo

The top 10 significant GO terms (based on *P* value) of differential expressed proteins in cell component (blue section), biological processes (red section), and molecular function (green section). Terms of the different categories are ordered by *P* values.

in binding functions include actin binding, phospholipid, collagen, cadherin, and glutathione binding, followed by phospholipase inhibitor activity and oxidoreductase activity.

Interestingly, both of the up-regulated and down-regulated proteins shared several common enrichment terms, such as the neutrophil degranulation term for BP, extracellular region, exosome, adhesion, and granular lumen terms for CC, and oxidoreductase activity for MF.

To uncover DEPs-associated pathways, KEGG pathway enrichment analysis was conducted with DAVID. As shown in Figure 4, DEPs associated with the cargo concentration in the ER, oxidatively deaminated to aldehydes by monoamine oxidase A (MAOA) and monoamine oxidase B (MAOB), eukaryotic translation termination, amino acid synthesis, vesicle biogenesis with transport, detoxification of reactive oxygen species (ROS), and formyl peptides binding.

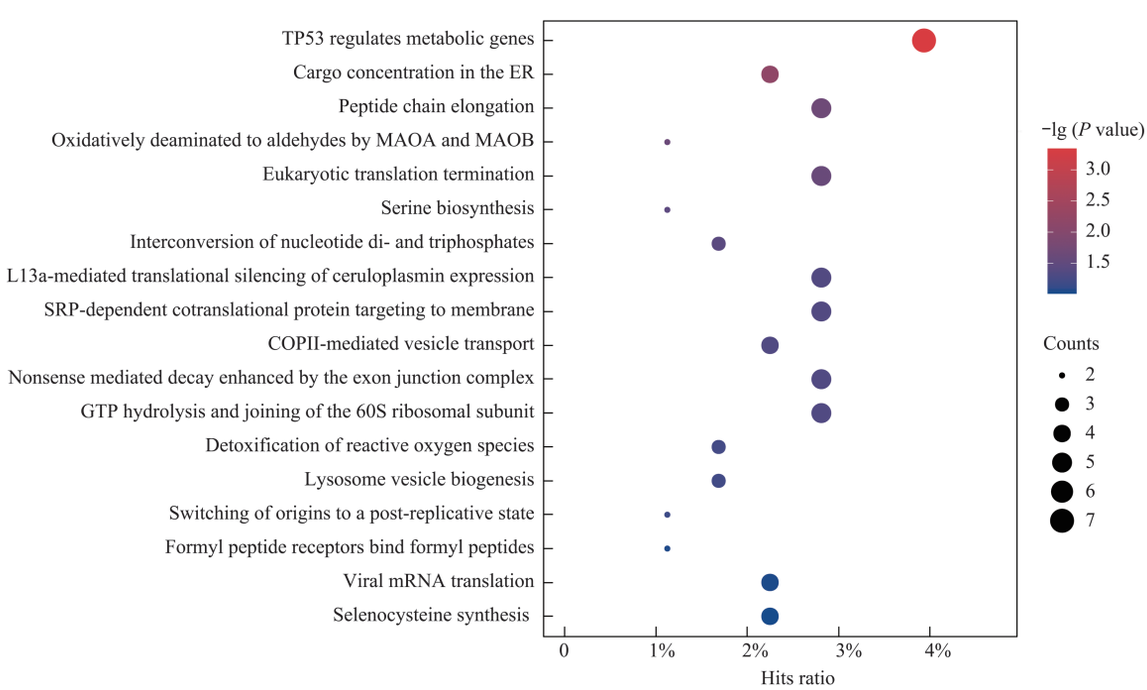

Fig. 4　KEGG pathway analysis of DEPs in epidermis of vitiligo

The pathways are ordered by *P* values, the size of the dots represents the number of genes, and the color of the dots represents the *P* value.

2.4 Protein-protein interaction （PPI） network construction

PPI network of DEPs was performed by STRING online database (Version 11.5). Each node represents a protein, color in nodes represents different GO functions (red for metabolic process, green for oxidation-reduction process, purple for immune system process, yellow for cell adhesion). The edge represents protein-protein interaction, different colors of edges indicate different functional and physical protein associations. PPI network construction carried out under the condition of minimum required interaction score was 0.4 (medium confidence). As shown in Figure 5, 180 nodes (only nodes with interactions were shown) with 102 edges were found (PPI enrichment *P* value: < 4.16×10^{-8}). Functional enrichments analysis shows that among the 181 DEPs there are 119 proteins involved in the metabolic process, 42 proteins involved in immune system process, 27 proteins take part in the oxidation-reduction process, and 15 proteins involve in cell adhesion. The multicolored nodes and edges obviously indicate that there is a close relationship between the different protein clusters. These multicolored proteins with high interaction scores (≥0.7) need further analysis. These proteins include PRDX1, PRDX2, EEF2, ITGB1, SPTBN2, ANXA1, and PFKL, and may play an important role in the pathogenesis of vitiligo.

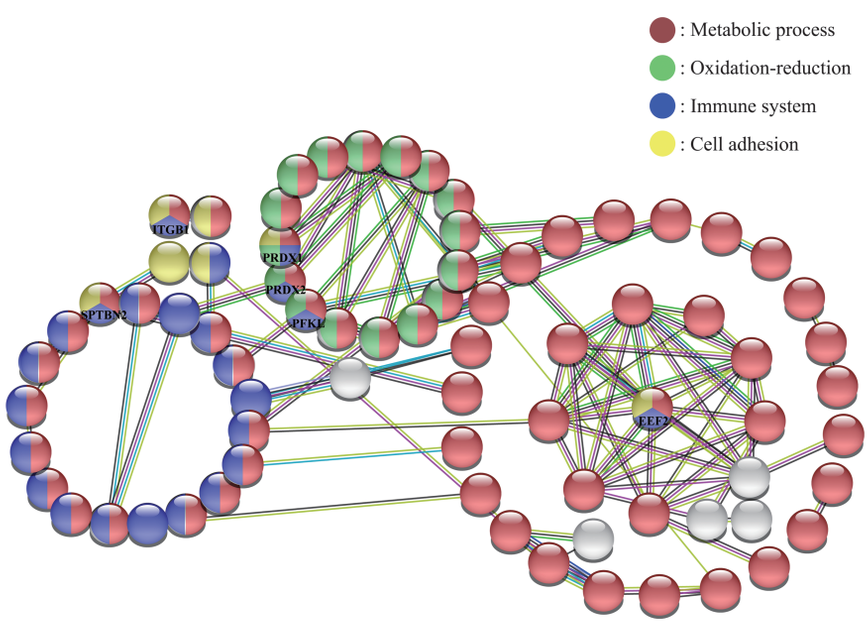

Fig. 5　Protein-protein interaction network of DEPs

STRING (Version 11.5) online database was used. Each node represents a protein, color in nodes represents different GO term (red for metabolic process, green for oxidation-reduction process, purple for immune system process, yellow for cell adhesion, white for another process). An edge represents protein-protein interaction, different color of edges indicate different functional and physical protein associations. PPI network construction carried out under the condition of minimum required interaction score was 0.4 (medium confidence).

2.5 Gene set enrichment analysis

We also analyzed the gene set enrichment network of all quantified proteins (including changed and unchanged) by GSEA (Gene set enrichment analysis 4.1.0), and analysis was visualized with Cytoscape (Version: 3.8.2). Applying the thresholds (*P* value<0.05, *FDR*<5%) as cutoff criteria. As shown in Figure 6, a total of 315 gene sets (nodes represent gene sets) were found and most of the down-regulated gene-sets clustered to immune response, followed by cell adhesion, migration, junction, wound healing, endocytosis, and lipid transport, whereas all the clusters but lipid transport above were related with each other (edges represent overlap). The upregulated gene sets were involved in macromolecules (including DNA, RNA, protein) metabolism, keratinization, and oxidant detoxification.

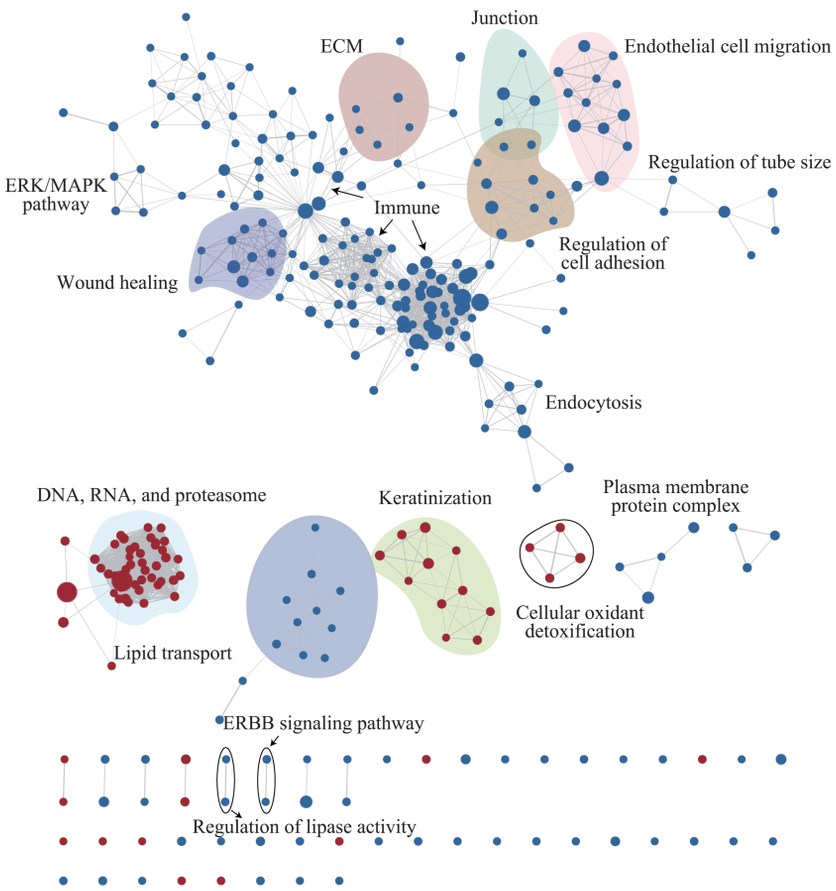

Fig. 6　GSEA enrichment map of vitiligo LE *vs* NLE

Nodes represent gene-sets and edges represent GSEA defined relations (overlapped genes in each sets), red nodes represents up-regulated gene sets whereas blue represents down-regulated gene sets. The gene sets circled in irregular shapes were represents a cluster of gene sets where the gene sets have the same enriched GO terms.

3　Discussion

3.1　Enhanced keratinization （cornification） in LE

Physiological skin protection against UV radiation damage includes stimulation of melanin synthesis, enhanced keratinization, and increasing the antioxidant activity[11].

In the current study, GO and GSEA analysis shows that keratinization is enhanced in LE compared to the NLE. GO analysis enriched keratinization associated proteins include Keratin76 (KRT76), Keratin16 (KRT16), Caspase-14 (CASP14), and Lipase member N (LIPN), while KRT76 is the highest expressed protein in LE. KRT76 is a type II cytoskeletal intermediate filament protein that protects epithelial cells from both mechanical and non-mechanical stresses[12]. Another significantly up-regulated keratin is KRT16, which is reported to contribute to hyperproliferation, cell adhesion, and migration[13]. CASP14 is a different caspase family member that is activated in the normal keratinization process without activating apoptosis[14]. LIPN is involved in the last step of keratinocyte differentiation and lipid metabolism[15]. In all, we speculated that these four proteins participate in the process of keratinization and play important role in protecting the skin from the UV radiation.

3.2　Lipid metabolism in LE

STRING online database analysis showed that most of DEPs were involved in the metabolic process, and 25 DEPs were lipid-associated proteins. GSEA analysis also showed a cluster of gene sets associated with lipid metabolism. So, we investigated these lipid-associated proteins in detail. Fatty acid-binding protein 5 (FABP5) is one of the significantly

up-regulated proteins in LE. FABP5 is a class of cytosolic lipid-binding protein that controls hydrophobic lipids transport and metabolism[16-17]. Overexpression of FABP5 enhances lipid metabolism, mediating uptake of fatty acids and reducing the levels of cellular free fatty acid[18]. Up-regulation of FABP5 may imply that LE has greater fatty acid uptake and enhanced lipid metabolism than NLE. Apolipoprotein C1 (APOC1) inhibits lipoprotein binding with low-density lipoprotein (LDL) receptor, very-low-density lipoprotein (VLDL) receptor, and LDL receptor-related protein (LRP) [19]. Only basal layer keratinocyte expresses the LDL receptors[20-21]. APOC1 affects the lipid composition of the epidermis[22]. In our study, we found APOC1 down-regulated in LE, indicating more LDL uptake into basal keratinocytes. Besides, we found that Acetyl-CoA acetyltransferase (ACAT1) is also down-regulated in LE, resulting in more free cholesterol and fewer cholesterol esters in keratinocytes.

From analysis above, we speculated that there is increased lipid uptake and metabolism in LE vitiligo than NLE vitiligo. The lipid metabolic difference in LE might be essential for the keratinization that supplies the energy source for proliferation, and maybe the change in the epidermis lipid composition by APOC1 offer more UV protection than NLE.

3.3 Immunity in LE

GSEA analysis and STRING PPI analysis indicated that another group of proteins related with vitiligo was immunity The highest enriched gene sets function in GSEA analysis was immunity. 42 DEPs involved in the immune system process from STRING PPI analysis, among which 4 T-cell enriched proteins (overlapped with TOP 100 T-cell enriched proteins[23]) were identified, including POSTN, APOH, F5, and ARG1. POSTN, APOH and F5 were down-regulated which may indicate decreased amount of T-cell in LE. ARG1 is implicated in immunosuppressive processes, up-regulated ARG1 in LE suggests less immunity in LE[24-27]. Moreover, the elevated ARG1 level stimulates keratinocyte proliferation[27-28].

In all, we assume that LE in stable vitiligo exhibits less immune activity than NLE. That is probably the cause of the diminished melanocytes in LE, as melanocytes are the source of inflammation, apoptosis, and recruited immune cells.

3.4 Amine oxidases （MAOs） in LE and NLE

KEGG pathway analysis shows that DEPs are involved in deaminated aldehydes by MAOA and MAOB. MAOs (MAOA and MAOB) are involved in the metabolism of dopamine, therefore MAOs closely are associated with neurodegenerative disorders[29-31]. In addition, dopamine and melanin synthesis share the same preprocess[32]. In our study, we found down-regulated MAOA and up-regulated MAOB in LE, indicating that vitiligo pathogenesis is associated with neurotransmitters.

Nerve endings and keratinocytes release noradrenaline into the epidermal microenvironment that inhibits tyrosinase (vital enzyme in melanin synthesis) activity in epidermal melanocytes[33]. In addition, MAOA especially degrades noradrenaline[34]. The previous study showed that the expression levels of MAOs was lower in lesional skin than non-lesional in active vitiligo[32]. In our study, we found down-regulated MAOA in LE. These findings indicate that down-regulated MAOA may be one of the reasons for disappeared melanin in LE.

In conclusion, down-regulated MAOA and up-regulated MAOB in LE could be the promising marker of stable vitiligo and could also be one of the reasons for the disappearance of melanin in LE. Probably the evidence for vitiligo pathogenesis associated with neurotransmitters.

3.5 Oxidoreduction in LE

All of GO, KEGG, STRING, and GSEA analysis shows an enriched function on the oxidoreduction system. An abnormal oxidoreduction system is responsible for oxidative stress. Oxidative stress is caused by an imbalance between the reactive oxygen species (ROS) formation and the antioxidant ability to reduce these reactive intermediates[35]. Oxidative stress has been demonstrated to play a major role in the onset and progression of vitiligo[36-37]. Antioxidant activity is one of the important physiological skin protection against UV radiation[11]. The epidermis of vitiligo patients exhibits a high level of ROS and reduced antioxidant capacity[36, 38-39]. In this study, we identified 33 antioxidants-related proteins some well-known antioxidants (SOD, CAT, HO, GPXs) displayed no expression changes in LE and NLE, however, several antioxidant-related proteins were up-regulated (KEAP1, GLRX, PRDX1, PRDX2, TXNDC17, TXNDC5) and down-regulated (GSR,

GSTM2, GSTM3). These proteins are an important regulator of the redox system, among which, GLRX, GSR, GSTM2, and GSTM3 are essential for the proper functioning the glutathione (GSH) that is a main non-enzymatic thiol-containing antioxidant in mammalian cells[40]. PRDX1, PRDX2, TXNDC17, and TXNDC5 are the other different antioxidant system that plays pivotal roles in regulating multiple cellular redox processes[41-42]. Keap1 is a critical component of the Keap1-Nrf2 pathway, acting as antioxidants by sensing oxidative stress and regulating Nrf2 activity[43]. Normally Keap1 over-expression leads the Nrf2 to be less translocated into nucleus and decreases the expression of target genes[44] (target genes include PRDX1, GSR, GSTM2, GSTM3, GCLC, and HO1). Actually, differential expression levels of downstream target genes in our study indicate that these antioxidants may not only be targeted by Nrf2.

Furthermore, each of these differentially expressed antioxidants-related proteins are involved in many other processes apart from the antioxidation process. Several reports showed that GSR negatively correlates with UVA radiation[11, 37, 45]. Overexpressed GLRX inhibits oxidative stress and apoptosis[46], performing a suppressive role in the immune response[47]. In our study, STRING PPI online analysis shows that PRDX1 and PRDX2 are associated with immune and metabolic processes. So, we conclude that LE and NLE have different redox levels.

4 Conclusion

The comparative proteomic study revealed that there were functional differences in keratinization, immunity, lipid metabolism and redox between LE and NLE in vitiligo patients. PRDX1, PRDX2, EEF2, ITGB1, SPTBN2, ANXA1 and PFKL were found as the key proteins to disfunction of LE.

Supplementary Available online (http://www.pibb.ac.cn or http://www.cnki.net):
PIBB_20220158_Fig S1.tif
PIBB_20220158_Fig S2.tif
PIBB_20220158_File S1.pdf
PIBB_20220158_Table S1.xlsx

References

[1] Frisoli M L, Essien K, Harris J E. Vitiligo: mechanisms of pathogenesis and treatment. Annu Rev Immunol, 2020, **38**:621-648

[2] Zubair R, Hamzavi I H. Phototherapy for vitiligo. Dermatol Clin, 2020, **38**(1): 55-62

[3] Katz E L, Harris J E. Translational research in vitiligo. Front Immunol, 2021, **12**: 624517

[4] Bishnoi A, Parsad D. Clinical and molecular aspects of vitiligo treatments. Int J Mol Sci, 2018, **19**(5): 1509

[5] Shen S, An B, Wang X, *et al*. Surfactant cocktail-aided extraction/precipitation/on-pellet digestion strategy enables efficient and reproducible sample preparation for large-scale quantitative proteomics. Anal Chem, 2018, **90**(17): 10350-10359

[6] Chen C, Geng L, Xu X, *et al*. Comparative proteomics analysis of plasma protein in patients with neuropsychiatric systemic lupus erythematosus. Ann Transl Med, 2020, **8**(9): 579

[7] Vasquez-Canizares N, Wahezi D, Putterman C. Diagnostic and prognostic tests in systemic lupus erythematosus. Best Pract Res Clin Rheumatol, 2017, **31**(3): 351-363

[8] Li Y L, Qi R Q, Yang Y, *et al*. Screening and identification of differentially expressed serum proteins in patients with vitiligo using twodimensional gel electrophoresis coupled with mass spectrometry. Mol Med Rep, 2018, **17**(2): 2651-2659

[9] Li Q, Lv Y, Li C, *et al*. Vitiligo autoantigen VIT75 is identified as lamin A in vitiligo by serological proteome analysis based on mass spectrometry. J Invest Dermatol, 2011, **131**(3): 727-734

[10] Li J, Chen X, Yi J, *et al*. Identification and characterization of 293T cell-derived exosomes by profiling the protein, mRNA and microRNA components. PLoS One, 2016, **11**(9): e0163043

[11] Rysava A, Cizkova K, Frankova J, *et al*. Effect of UVA radiation on the Nrf2 signalling pathway in human skin cells. J Photochem Photobiol B, 2020, **209**: 111948

[12] Liakath-Ali K, Vancollie V E, Heath E, *et al*. Novel skin phenotypes revealed by a genome-wide mouse reverse genetic screen. Nat Commun, 2014, **5**: 3540

[13] Zhang X, Yin M, Zhang L J. Keratin 6, 16 and 17-critical barrier alarmin molecules in skin wounds and psoriasis. Cells, 2019, **8**(8): 807

[14] Lippens S, Denecker G, Ovaere P, *et al*. Death penalty for keratinocytes: apoptosis versus cornification. Cell Death Differ, 2005, **12**:1497-1508

[15] Toulza E, Mattiuzzo N R, Galliano M F, *et al*. Large-scale identification of human genes implicated in epidermal barrier function. Genome Biol, 2007, **8**(6): R107

[16] O'sullivan S E, Kaczocha M. FABP5 as a novel molecular target in prostate cancer. Drug Discov Today, 2020, **25**(11): 2056-2061

[17] Thumser A E, Moore J B, Plant N J. Fatty acid binding proteins:

tissue-specific functions in health and disease. Curr Opin Clin Nutr Metab Care, 2014, **17**(2): 124-129

[18] Hotamisligil G S, Bernlohr D A. Metabolic functions of FABPs--mechanisms and therapeutic implications. Nat Rev Endocrinol, 2015, **11**(10): 592-605

[19] Muurling M, Van Den Hoek A M, Mensink R P, *et al*. Overexpression of APOC1 in obob mice leads to hepatic steatosis and severe hepatic insulin resistance. J Lipid Res, 2004, **45**(1): 9-16

[20] Mommaas M, Tada J, Ponec M. Distribution of low-density lipoprotein receptors and apolipoprotein B on normal and on reconstructed human epidermis. J Dermatol Sci, 1991, **2**(2): 97-105

[21] Mommaas-Kienhuis A M, Grayson S, Wijsman M C, *et al*. Low density lipoprotein receptor expression on keratinocytes in normal and psoriatic epidermis. J Invest Dermatol, 1987, **89**(5): 513-517

[22] Jong M C, Gijbels M J, Dahlmans V E, *et al*. Hyperlipidemia and cutaneous abnormalities in transgenic mice overexpressing human apolipoprotein C1. J Clin Invest, 1998, **101**(1): 145-152

[23] Dyring-Andersen B, Løvendorf M B, Coscia F, *et al*. Spatially and cell-type resolved quantitative proteomic atlas of healthy human skin. Nat Commun, 2020, **11**(1): 5587

[24] Fernandes T L, Gomoll A H, Lattermann C, *et al*. Macrophage: a potential target on cartilage regeneration. Front Immunol, 2020, **11**: 111

[25] Grzywa T M, Sosnowska A, Matryba P, *et al*. Myeloid cell-derived arginase in cancer immune response. Front Immunol, 2020, **11**: 938

[26] Wang H, Ji J, Zhuang Y, *et al*. PMA induces the differentiation of monocytes into immunosuppressive MDSCs. Clin Exp Immunol, 2021, **206**(2): 216-225

[27] Weber C, Telerman S B, Reimer A S, *et al*. Macrophage infiltration and alternative activation during wound healing promote MEK1-induced skin carcinogenesis. Cancer Res, 2016, **76**(4): 805-817

[28] Redmond A F, Rothberg S. Arginase activity and other cellular events associated with epidermal hyperplasia. J Cell Physiol, 1978, **94**(1) :99-104

[29] Kolla N J, Bortolato M. The role of monoamine oxidase A in the neurobiology of aggressive, antisocial, and violent behavior: a tale of mice and men. Prog Neurobiol, 2020, **194**: 101875

[30] Salvatore J E, Dick D M. Genetic influences on conduct disorder. Neurosci Biobehav Rev, 2018, **91**: 91-101

[31] Emamzadeh F N, Surguchov A. Parkinson's disease: biomarkers, treatment, and risk factors. Front Neurosci, 2018, **12**: 612

[32] Reimann E, Kingo K, Karelson M, *et al*. Expression profile of genes associated with the dopamine pathway in vitiligo skin biopsies and blood sera. Dermatology, 2012, **224**(2): 168-176

[33] Lan W J, Wang H Y, Lan W, *et al*. Geniposide enhances melanogenesis by stem cell factor/c-Kit signalling in norepinephrine-exposed normal human epidermal melanocyte. Basic Clin Pharmacol Toxicol, 2008, **103**(1): 88-93

[34] Saglik B N, Osmaniye D, Acar Cevik U, *et al*. Synthesis, *in vitro* enzyme activity and molecular docking studies of new benzylamine-sulfonamide derivatives as selective MAO-B inhibitors. J Enzyme Inhib Med Chem, 2020, **35**(1): 1422-1432

[35] Poprac P, Jomova K, Simunkova M, *et al*. Targeting free radicals in oxidative stress-related human diseases. Trends Pharmacol Sci, 2017, **38**(7): 592-607

[36] Fang W, Tang L, Wang G, *et al*. Molecular hydrogen protects human melanocytes from oxidative stress by activating Nrf2 signaling. J Invest Dermatol, 2020, **140**(11): 2230-2241.e2239

[37] Tang S, Yang L, Kuroda Y, *et al*. Herb Sanqi-derived compound K alleviates oxidative stress in cultured human melanocytes and improves oxidative-stress-related leukoderma in Guinea pigs. Cells, 2021, **10**(8): 2057

[38] Ahn Y, Seo J, Lee E J, *et al*. ATP-P2X7-induced inflammasome activation contributes to melanocyte death and CD8(+) T-cell trafficking to the skin in vitiligo. J Invest Dermatol, 2020, **140**(9): 1794-1804.e4

[39] Li S, Zhu G, Yang Y, *et al*. Oxidative stress drives CD8(+) T-cell skin trafficking in patients with vitiligo through CXCL16 upregulation by activating the unfolded protein response in keratinocytes. J Allergy Clin Immunol, 2017, **140**(1): 177-189. e179

[40] Yin Y, Xu N, Qin T, *et al*. Astaxanthin provides antioxidant protection in LPS-induced dendritic cells for inflammatory control. Mar Drugs, 2021, **19**(10): 534

[41] Zhang J, Li X, Han X, *et al*. Targeting the thioredoxin system for cancer therapy. Trends Pharmacol Sci, 2017, **38**(9): 794-808

[42] Szeliga M. Peroxiredoxins in neurodegenerative diseases. Antioxidants (Basel), 2020, **9**(12): 1203

[43] Yu C, Xiao J H. The Keap1-Nrf2 system: a mediator between oxidative stress and aging. Oxid Med Cell Longev, 2021, **2021**: 6635460

[44] Zhao X J, Yu H W, Yang Y Z, *et al*. Polydatin prevents fructose-induced liver inflammation and lipid deposition through increasing miR-200a to regulate Keap1/Nrf2 pathway. Redox Biol, 2018, **18**: 124-137

[45] Nechifor M T, Dinu D. 3-Amino-1,2,4-triazole limits the oxidative damage in UVA-irradiated dysplastic keratinocytes. Biomed Res Int, 2017, **2017**: 4872164

[46] Sun J, Wei X, Lu Y, *et al*. Glutaredoxin 1 (GRX1) inhibits oxidative stress and apoptosis of chondrocytes by regulating CREB/HO-1 in osteoarthritis. Mol Immunol, 2017, **90**: 211-218

[47] Chang Y, Li G, Zhai Y, *et al*. Redox regulator GLRX is associated with tumor immunity in glioma. Front Immunol, 2020, **11**: 580934

白癜风患者病变表皮与正常表皮的比较蛋白质组学研究*

艾力克木·吐尔逊[1,2,3)]　陈秀兰[2,3)]　艾尼瓦尔·塔力甫[4)]　李　娜[2,3)]　王继峰[3)]　蔡潭溪[2,3)]
郭晓静[2,3)]　丁　翔[3)]　谢振声[3)]　牛丽丽[3)]　张朦朦[3)]　Ghulam　Abbas[2,3)]
阿吉艾克拜尔·艾萨[1,2)**]　杨福全[2,3)**]

([1)] 中国科学院新疆理化技术研究所干旱区植物资源化学重点实验室，乌鲁木齐 830011；[2)] 中国科学院大学，北京 100049；
[3)] 中国科学院生物物理研究所，北京 100101；[4)] 新疆维吾尔自治区维吾尔医医院，乌鲁木齐 830049）

摘要　目的　本文通过开展白癜风患者病变表皮与正常表皮的比较蛋白质组学研究，发现和鉴定白癜风患者病变表皮与正常表皮之间的差异表达蛋白，以探讨白癜风患者表皮发生病变的分子机制。**方法**　首先，建立和优化了表皮样品中蛋白质的最佳酶切条件。其次，采用基于串联质谱标签（TMT）标记的定量蛋白质组学技术策略开展了稳定期白癜风患者病变表皮与正常表皮的比较蛋白质组学研究，并筛选了差异表达蛋白。最后通过生物信息学分析工具及数据库（GO、KEGG、STRING、GSEA）对差异蛋白进行功能富集分析。**结果**　优化所得到的最佳酶解条件是由Lys-C（酶：底物，1：100）和胰酶（酶：底物，1：50）组合而成的顺序酶切。比较蛋白质组学研究共鉴定4 496个蛋白质，其中181个蛋白质为白癜风患者病变表皮中的差异表达蛋白。生物信息学分析表明差异表达蛋白主要与代谢、免疫、氧化还原和细胞黏附相关。其中119个上调蛋白主要参与角质化、转录、氧化应激及蛋白酶解等过程。62个下调蛋白主要参与细胞内物质运输、谷胱甘肽代谢和肌动蛋白细丝封端等过程。**结论**　比较蛋白质组学研究揭示了白癜风患者病变表皮与正常表皮之间主要存在角质化、免疫、脂质代谢和氧化还原等方面的功能差异，发现了PRDX1、PRDX2、EEF2、ITGB1、SPTBN2、ANXA1及PFKL等蛋白质为潜在的白癜风患者病变表皮功能失调的关键蛋白质。

关键词　白癜风，表皮蛋白组学，TMT标记定量，角质化，氧化应激，脂质代谢
中图分类号　Q51，Q594　　**DOI**：10.16476/j.pibb.2022.0158

* 国家重点研发计划（2020YFE0205600）资助项目。
** 通讯联系人。
杨福全　Tel：010-64888581，E-mail：fqyang@ibp.ac.cn
阿吉艾克拜尔·艾萨　Tel：0991-3835679，E-mail：haji@ms.xjb.ac.cn
收稿日期：2022-04-11，接受日期：2022-05-09